

## STEREO PARTICLE SHADOW VELOCIMETRY FOR TURBULENT FLOW CHARACTERIZATION

### Jeff Harris

Fluids Research Department  
Applied Research Laboratory  
Pennsylvania State University  
University Park, PA, USA  
jeff.harris@psu.edu

### Michael McPhail

Center for Regenerative Medicine  
Mayo Clinic  
Scottsdale, AZ, USA

### Christine Truong

Applied Research Laboratory  
Pennsylvania State University  
University Park, PA, USA

### Zachary Berger

Flow Acoustics Department  
Applied Research Laboratory  
Pennsylvania State University  
University Park, PA, USA

### ABSTRACT

Particle shadow velocimetry (PSV) is an optical, LED-based flow diagnostic technique that images a backlit flow field and uses inverted images to quantify the velocity. The planar, two-component version of this measurement technique has been shown to produce reasonably accurate results up to third and fourth order statistics. The aim of this work is to show that the turbulent spectra and reduced order modeling analysis from PIV data are comparable to the same measured with PSV. This type of analysis has never been done on a stereoscopic PSV measurement, so the limitations of such analysis for this measurement technique should be demonstrated. The flow field of a small jet is measured using stereo PIV and stereo PSV and the through-plane velocity is compared. A second test using a fully-developed pipe flow in glycerin is used to analyze the velocity mean, variance, and the temporal and spatial spectra for each measurement at several locations. Reduced order modeling in the form of proper orthogonal decomposition is also used to analyze and filter the noise in the measurements.

### INTRODUCTION

This paper describes stereoscopic particle shadow velocimetry (SPSV), which stems from a proven technique of planar particle shadow velocimetry (PSV). Stereo PSV measures three components of velocity in a thin plane, similar to stereoscopic particle image velocimetry (SPIV). Both techniques yield fluid field velocities by first imaging small tracer particles in a flow field. Displacement fields are computed from the cross-correlation of two subsequent images of the particles. Three components of velocity can be measured in a planar region by imaging the flow field with two cameras in a stereoscopic setup. Two-component PIV, and its stereoscopic variant, SPIV described by Prasad (2000), use a high intensity light sheet to illuminate the flow field.

Cameras then image the scattered light from the particles to compute the fluid motion. In PSV, introduced by Goss & Esteveordal (2006), the camera images the light field generated by overdriven pulsed light emitting diodes (LEDs) and the shadows cast by the tracer particles. The PSV images are, in essence, inverted to provide a dark background with bright particles for the standard cross-correlation algorithms commonly used in PIV.

Previous works have demonstrated PSV in two-dimensional applications (Chételat & Kim, 2002; Goss & Esteveordal, 2006; Goss *et al.*, 2007; McPhail *et al.*, 2015a), for measurement of two-dimensional unsteady acceleration (McPhail *et al.*, 2015b), for micro-PSV (Khadaparast *et al.*, 2013), and for tomographic measurement (Aguirre-Pablo *et al.*, 2017). LEDs have also been used for velocimetry measurements in front-lit micro-PIV setup (Hagsäter *et al.*, 2008), to form a light sheet for PIV (Willert *et al.*, 2010), in a side-scatter tomographic PIV (Buchmann *et al.*, 2012), and in conjunction with PIV in multiphase flows (Lindken & Merzkirch, 2002). The use of backlighting makes PSV a useful alternative to PIV when there is not optical access for a laser sheet or for other scenarios where a laser is less ideal. Dynamic range can also be improved through the use of multicolor LEDs and a color camera (McPhail *et al.*, 2015b). It is noted that PSV should be considered as another tool in the suite of optical flow diagnostic techniques rather than a replacement for PIV. This work aims to demonstrate that the tool can provide a dataset of comparable quality to PIV. This comparison would also make apparent the limitations of PSV compared to PIV, with the primary difference being the depth of field and related complications from conducting a planar measurement with a nearly volumetric image.

The measurement volume thickness in volumetric illumination techniques such as PSV and micro-PIV, called the depth of correlation (DOC), is set by the imaging optics (Meinhart *et al.*, 2000; Olsen & Adrian, 2000). This depth

can be a limitation on the PSV measurement technique and its effects can be characterized in a planar setup. The effects of this depth and the image processing compared to PIV in a stereoscopic measurement would be included in the source of difference in the presented results. An analysis of the DOC is not explicitly included herein (see Truong *et al.* (2018a)).

Two tests are presented, each with slightly different goals. The first is a small jet placed in a water box. The jet flowed at an angle through the illumination plane, providing a through-plane component of velocity. This test allowed the comparison of mean and standard deviations of the stereo PSV with the stereo PIV. There were several limitations to this test, so a second test was conducted to allow for higher order statistics to be compared and to mitigate the limitations found in the small jet test. The second test consisted of a nearly simultaneous acquisition of planar and stereo PIV and PSV in a fully-developed pipe flow of glycerin. This canonical flow gives a deeper comparison of statistics that can be used to benchmark stereo PSV with the other measurement techniques and allows for comparisons of planar measurements to stereo measurements using simultaneously acquired images.

## EXPERIMENT

Two different tests are presented and each have a slightly different goal. First, a small jet experiment was conducted to characterize a non-uniform and significant through-plane velocity measured by both stereo PIV (SPIV) and stereo PSV (SPSV). The second test was conducted in a fully-developed pipe flow in glycerin to allow for simultaneous stereo PIV and PSV at high data rates to allow for comparison of higher order statistics and spectra.

### Jet Experiment

The schematic of the first test, the small jet inside of water box, is shown in Fig. 1. The tank was 25.4 cm × 50.8 cm (10 in × 20 in) with glass sidewalls. A small pump was placed in the tank to generate a circular jet. The hardware was arranged so that SPIV and SPSV data could be acquired in the same nominal field of view without adjusting the cameras and the camera calibration. Flow seeding was provided by 45-105 μm EconoStar 106 Cenosphere particles. Custom prisms were made to improve image quality, as sketched in Fig. 1. The walls of the prisms were made of acrylic fixed to the outside wall of the tank using room temperature vulcanization silicone. The prisms were then filled with water. The surface of the prisms formed an approximately 21° angle with the outer surface of the fish tank.

Two v311 Phantom (Vision Research) cameras were used for imaging fitted with Scheimpflug lens mounts and 200mm Nikon lenses. A dual laser-head, solo-PIV Nd:YAG laser (New Wave Research) was used for SPIV illumination. A cylindrical lens on the laser head formed the laser light sheet. A bank of overdriven LEDs from Innovative Scientific Solutions Incorporated with a set pulse width of 5 μs was used for SPSV illumination in a small-band wavelength (blue light only). A blank sheet of paper was placed between the LED bank and the water tank to provide an even distribution of light. DaVis 8.3.0 (LaVision GmbH) was used to acquire data and control the laser and LED timing. Images were acquired at a rate of 12 Hz, with a dt of 300 μs between frames. Sets of 1500 images were acquired for each SPSV and SPIV dataset. A LaVision type 058-5

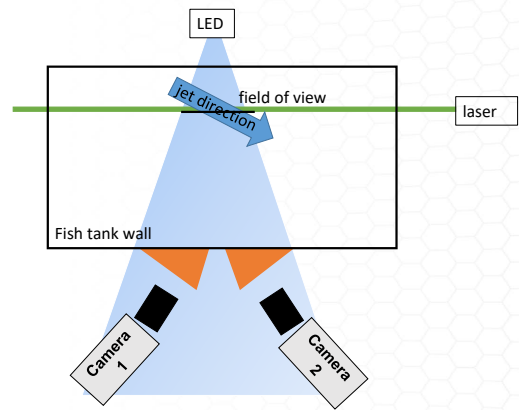


Figure 1: The stereo PSV and PIV setup showing the optical setup and jet flow direction.

two-level dot grid calibration plate was used for calibration and to dewarp the images.

This test had one primary limitation. The PIV and PSV data were not acquired simultaneously and the test was setup in a relatively small tank. The jet induced non-uniform circulation in the tank, which meant that datasets not acquired at the same time would not have precisely the same statistics. This test did, however, provide a suitable comparison of low order statistics (mean and standard deviation) of each of the three velocity components, with a non-zero mean in the through-plane component.

### Pipe Experiment

The second test utilized a fully-developed turbulent pipe flow in glycerin to provide a canonical flow field for benchmarking. The measurements can be compared to the standard literature, previous laser Doppler velocimetry (LDV) measurements, and simultaneous PIV measurements.

The flow of interest is a fully-developed pipe flow of glycerin. The 285 mm diameter glycerin tunnel at the Applied Research Lab at Penn State University has been used for many turbulence and benchmarking studies, starting with Bakewell Jr & Lumley (1967). Parameters such as velocity, viscosity, density, etc. vary with temperature, which is maintained at 37.8°C using a water-cooled heat exchanger. At this temperature, glycerin has a density of  $\rho = 1270 \text{ kg/m}^3$  and kinematic viscosity of  $\nu = 162 \times 10^{-6} \text{ m}^2/\text{s}$ . The Reynolds number of the flow is 8000 based on the tunnel radius  $r_{\text{tunnel}} = 14.25 \text{ cm}$  and peak mean velocity  $U(r_{\text{tunnel}}) = 9.0 \text{ m/s}$ . For further details of the facility, see Truong *et al.* (2018b), Chevrin *et al.* (1990), and Bakewell (1966).

Data is acquired in a 1.1 m long, 285 mm diameter clear acrylic test section 23 pipe diameters downstream of a trip ring following a contraction into the pipe inlet. The index of refraction of acrylic  $n_{\text{acrylic}} = 1.49$  closely matches that of glycerin  $n_{\text{glycerin}} = 1.47$ , allowing for optical measurements to be taken with low distortion. The test section outer wall is square but the inside surface is a smooth, circular pipe. Data were acquired away from the pipe wall, to mitigate effects of possible calibration errors due to the curvature of the wall.

Due to the large difference in the density of air compared to the density of glycerin, air bubbles are used as

seed particles because they are inherent to the glycerin and they have properties sufficient for optical measurements. The size these particles were measured holographically by Chevrin *et al.* (1990) to be 20-50  $\mu\text{m}$  in diameter. An estimate of Stokes number is several orders of magnitude less than 1.

Images were acquired using Phantom Camera Control 2.5 and two Phantom v311 cameras. One camera was placed perpendicular to the flow direction; the second was angled with respect to both the first camera and the flow. Both cameras were equipped with a 105-mm Nikon lens with  $f_{\#}=2.8$  (aperture completely open). A Scheimpflug mount and a glycerin-filled acrylic prism was used with the angled camera to minimize optical distortion. The exposure time for the perpendicular camera and the angled camera were 40  $\mu\text{s}$  and 400  $\mu\text{s}$ , respectively. A larger exposure time was necessary for the angled camera because of the scatter of laser light. The test setup is shown in Fig. 2. The top-down view is shown in Fig. 2a showing the measurement plane, layout of the cameras relative to the illumination sources. A downstream looking upstream view is shown in Fig. 2b, showing the location of the measurement plane in the radial direction.

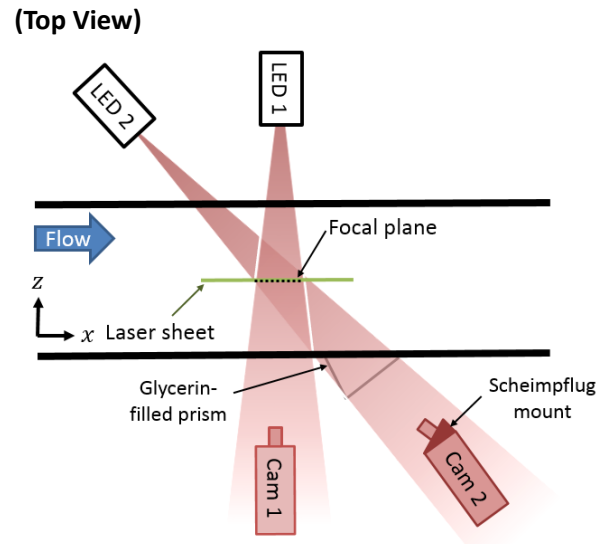
The laser and LED alternated in time to illuminate the flow field, so the particles in the flow reflect light in the PIV image and cast shadows in the PSV image. The cameras were given sufficient recovery time between PIV and PSV images so the CCD chip was not overexposed during measurement while maintaining a short time interval to claim that the data are simultaneous. A total of 11069 images were acquired in single-frame mode at sampling rate of 5000 Hz. The effective sampling rate between sequential PIV images (and sequential PSV images) was 2500 Hz and the time between frames was 400  $\mu\text{s}$ .

The images were calibrated using the same LaVision type 058-5 calibration plate. Third-order polynomial fits were used to calibrate the image. A self-calibration procedure described by Wieneke (2005) was applied to 100 measured SPIV images several times to correct for the spatial discrepancy between the laser sheet and calibration target. The distance between the target and the wall was determined by measuring the location of the calibration target with respect to the tunnel wall.

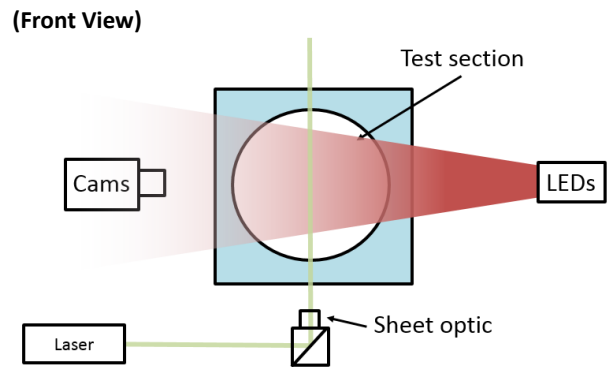
LaVision's DaVis v10.0.4 was used to process the images and corresponding velocity fields. A simple background subtraction was applied to SPIV images. A bright field correction with image length 5 and nonlinear strict sliding minimum filter with pixel length 3 was applied to SPSV images to remove noise and sharpen particle images. The 3-component velocity field was then computed using both camera images. The first pass was conducted with a  $64 \times 64$  square window with 50% overlap and a 50 px initial window shift. Three additional  $32 \times 32$  pixel circular windows with 50% overlap were then used to refine the velocity computation. Vector post-processing, such as vector filtering, were conducted using MATLAB R2017b. Turbulence statistics and spectral energy density were also calculated using MATLAB R2017b.

## RESULTS

The results for each of the two tests are considered individually in the following subsections.



(a) The stereo PSV and PIV setup at the glycerin tunnel viewed looking top-down, flow is left to right and camera 2 utilizes a Scheimpflug mount.



(b) The stereo PSV and PIV setup at the glycerin tunnel viewed looking along the axis of the pipe, flow coming out of page.

Figure 2: Two views of the stereo PIV/PSV setup in the glycerin tunnel.

## Jet Results

The velocity data for the small jet test is considered first. A contour plot of the velocity field is shown in Fig. 3. Two rows and two columns of data are extracted from the stereo PIV and stereo PSV fields (labeled R1, R2, C1, C2). The mean velocity profiles along these lines are plotted in Fig. 4 comparing the SPSV to the SPIV. The mean profiles for each of the velocity components show good agreement between the PIV and PSV. The standard deviation shows a slight difference between the two datasets, as shown in Fig. 5.

The relative difference between the PIV and the PSV standard deviation plots is shown in Fig. 6. The largest difference in the standard deviation is in the through-plane  $w$  component for a portion of the image. Most of the profile has a difference of the same percentage as the other two components of standard deviation. This statistic is often used to compute the turbulence intensity of a dataset, so agreement between the SPSV and SPIV shows that in many turbulence characterization measurements, SPSV may be a

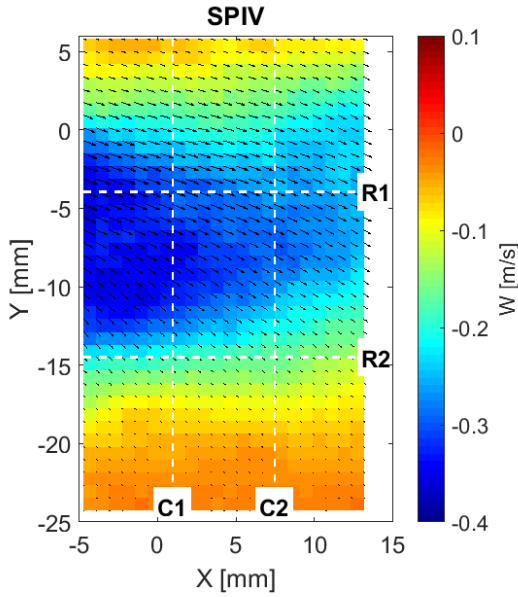


Figure 3: A velocity contour plot showing  $w$  with vectors showing the  $u, v$  components of velocity. Also shown are two rows and two columns where profiles were extracted and are shown in Fig. 4.

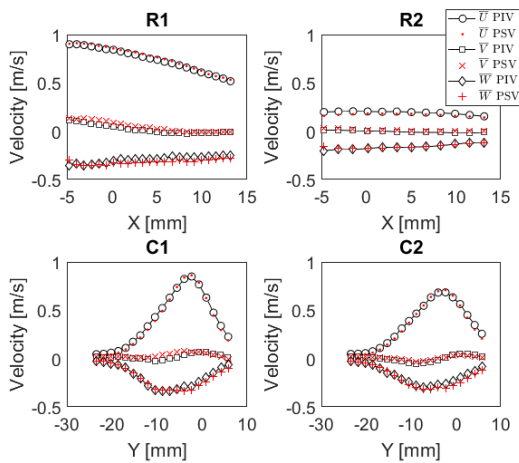


Figure 4: Mean velocity profiles showing all three components of velocity for the two measurement techniques.

suitable tool to consider if the standard SPIV acquisition is ill-suited.

From this test, all three components of mean velocity using SPIV and SPSV are the same. The standard deviation has some difference between the two techniques, but it is unclear if this was due to the measurement technique or limitations of the jet/water tank setup. The data were not acquired at the same time, so the flow field would have slight differences. This acquisition was also not time-resolved.

### Pipe Results

The mean profiles of the three components of velocity for planar and stereo PIV and PSV are shown in Fig. 7. These data are plotted in wall-coordinates with the shear velocity computed from measurements of the pressure drop

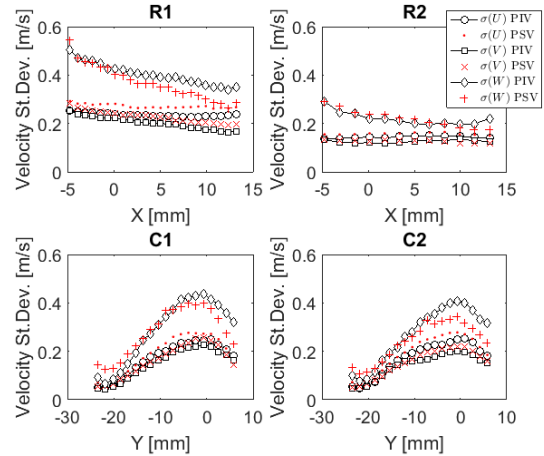


Figure 5: Standard deviation of velocity profiles showing all three components for the two measurement techniques.

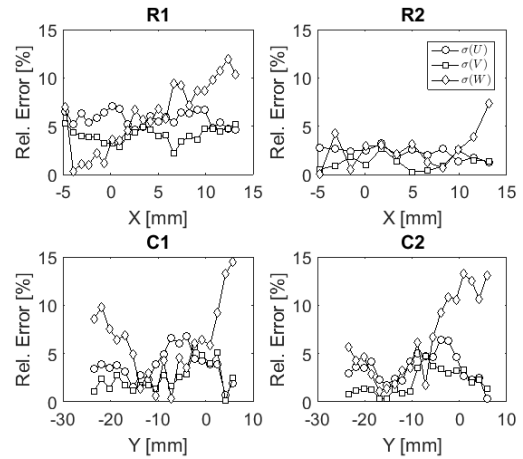


Figure 6: Relative difference of the standard deviation profiles from Fig. 5 showing all three components for the two measurement techniques.

along the pipe. These mean profiles are compared with LDV measurements of the same facility (see Fontaine & Deutsch (1993)). The difference between the planar PIV and the LDV profiles is 0.9% and the difference between the planar PSV and the LDV is 1.5%. The difference between the stereo PIV and the stereo PSV relative to the LDV is 1.6% and 2%, respectively. Figure 7 shows that the non-zero component of velocity for these measurements are all within good agreement, even with a less than ideal stereoscopic setup.

The standard deviation profiles in the pipe flow measured with planar PIV/PSV and stereo PIV/PSV are shown in Fig. 8, and these are also compared with the LDV data previously cited. The planar measurements are much less noisy compared to the LDV than the stereo measurements and the PIV and PSV are in very close agreement. The stereo data are further from the LDV measured standard deviation, but the PIV and PSV are both equally off together. This suggests that the overall stereo setup was less than optimal, but that the PIV and PSV report the same standard deviation in the streamwise component of velocity. Thus,

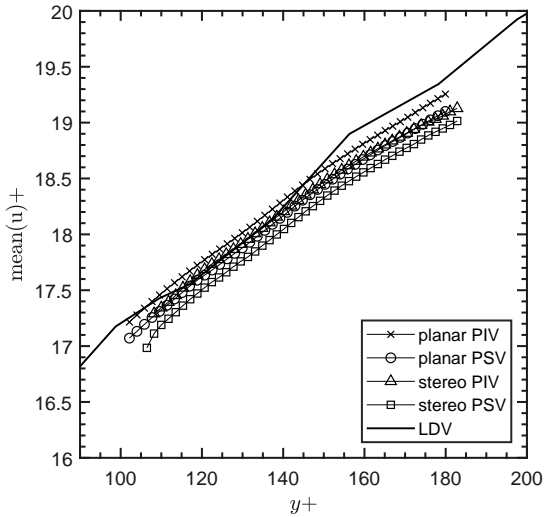


Figure 7: Mean velocity profiles showing axial velocity for planar PIV/PSV, stereo PIV/PSV and LDV.

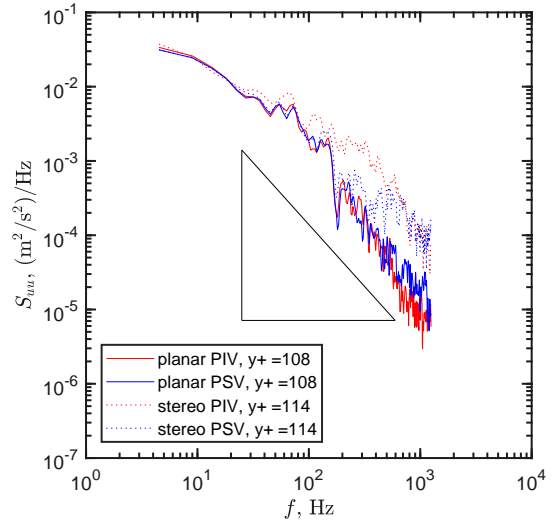


Figure 9: Axial power spectral density for planar PIV/PSV and stereo PIV/PSV.

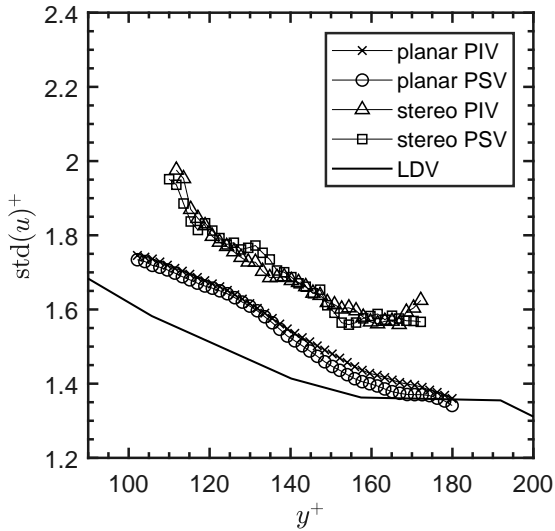


Figure 8: Standard deviation of axial velocity profiles for planar PIV/PSV, stereo PIV/PSV and LDV.

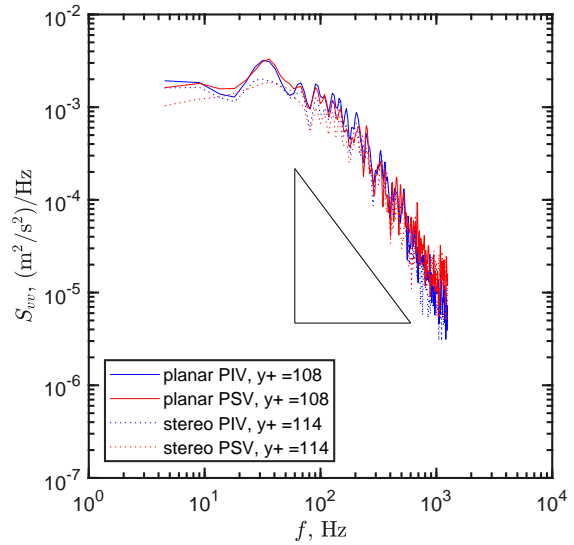


Figure 10: Radial velocity power spectral density for planar PIV/PSV and stereo PIV/PSV.

in a stereoscopic setup, PSV measurements are very similar to PIV measurements for a simple flow field such as the fully-developed pipe. Note that the jet test described above serves to demonstrate these low order statistics in a more useful fashion. These are merely presented for completeness and the focus of the pipe flow test will be on the spectra and POD reconstruction.

The power spectral density (PSD) of the measurements are computed for a fixed point away from the pipe wall. The PSD for the axial component of velocity is shown in Fig. 9. At low frequency, the measurement techniques show nearly identical frequency response. The PSD for the planar measurements are nearly identical for all measured frequencies, but the stereo measurement shows some discrepancy between the PIV and the PSV. In this location, the stereo PSV stays closer to the planar cases until around 400Hz and then joins the stereo PIV case as they approach a noise floor. The stereo measurements appear to have more noise than the planar measurements for this configuration.

The PSD of the radial component of velocity in Fig. 10 shows that the PIV and PSV spectra are in very close agreement in this component of velocity. The PIV appears to have a slightly lower noise floor, visible at the high frequencies.

The PSD for the through-plane component of velocity for the stereo data is shown in Fig. 11. This shows the expected trend of the PSV data reaching a slightly higher noise floor than the PIV. However, the PSV measurement closely matched the PIV measurement for most of the frequency range.

The figures above show that PSV will often have a slightly higher noise level than PIV. Generally, the trends resulting from SPSV are close to those measured from SPIV, but due to the often less-ideal image quality of the PSV image, may be more noisy. As the vector fields used to produce these results are not significantly post-processed, some advantage may be gained using a more strict filtering rou-

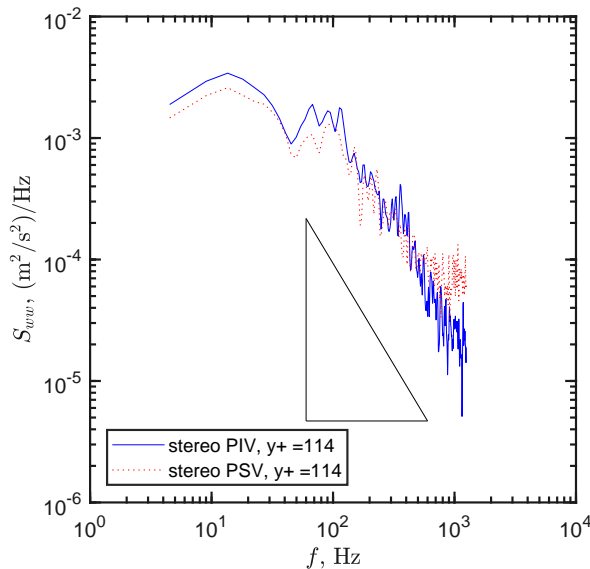


Figure 11: Power spectral density for through-plane velocity for stereo PIV/PSV.

tine.

Proper orthogonal decomposition (POD) was implemented in an attempt to filter noise from low energy modes from contaminating the desired measurement that is often apparent in the higher energy modes. Thus, the number of modes to reconstruct a velocity field containing 90% of the turbulence kinetic energy was used and the spectra resulting from that reconstruction is compared with the original PSD. The planar PIV comparison is shown in Fig. 12 where the reduced number of modes appears to decrease the noise level in the measurement (as it should). The planar PSV version of the same comparison is shown in Fig. 13. The PSV measurement has less benefit from filtering in this manner, suggesting that the noise is prevalent in even the higher energy modes.

The stereo PIV and PSV velocity spectra from the POD reconstruction is shown in Fig. 14. The removal of the low energy, noisy modes in the stereo data does reduce the noise seen in the PSV spectra. This suggests that a careful filtering of the PSV data is desired to bring the spectra into comparable levels with SPIV.

## CONCLUSIONS

Stereo PSV is a new measurement technique that requires a thorough benchmark and is compared to stereo PIV for that purpose. The comparison is done in a fully-developed pipe flow with glycerin as the working fluid for the comparison of spectral quantities. A simple through-plane jet test is also used to compare the mean and standard deviation of the 3 components of velocity.

The simple jet test with a through-plane component of velocity shows that the mean and standard deviation for a generic stereoscopic setup are in good agreement between the PIV and PSV techniques. The setup utilized a single light source for the backlighting, simplifying the setup. The measurement location was close enough to the side of the tank that this setup was possible. This data was acquired in a manner that limited comparison at high order statistics and of the spectra of the velocity components.

A different stereo setup in the glycerin tunnel pipe flow

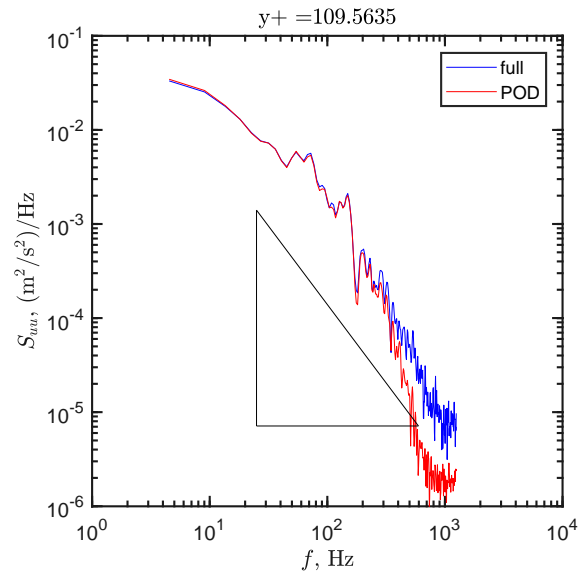


Figure 12: Power spectral density for the axial component of velocity for planar PIV comparing the spectra from the velocity data to that of a reduced mode reconstruction from POD.

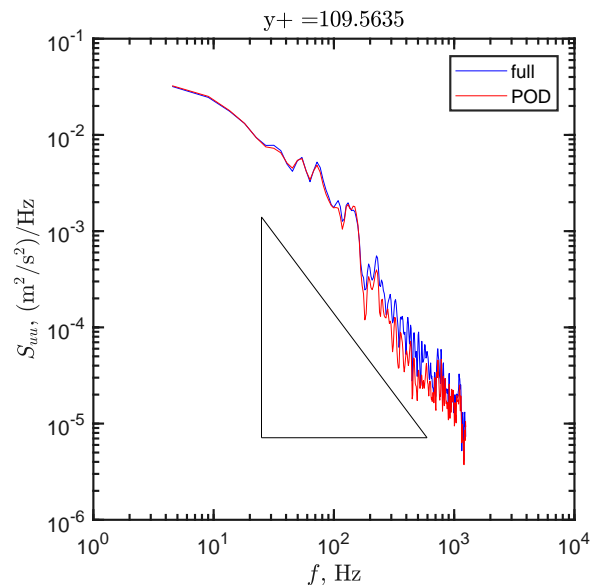


Figure 13: Power spectral density for the axial component of velocity for planar PSV comparing the spectra from the velocity data to that of a reduced mode reconstruction from POD.

was less ideal for multi-component measurement accuracy (given the zero mean of the through-plane component of velocity), but still provides a comparison between stereo PIV and stereo PSV for a simultaneous acquisition with planar versions of the same techniques using the same images. Overall, the stereo PSV agrees with stereo PIV in the power spectral density. Though the PSV measurement will have a little more noise or will have a higher noise floor. Careful filtering or POD can be used to reduce the measurement noise of the PSV measurements.

Generally speaking, if a certain aspect of the turbulent

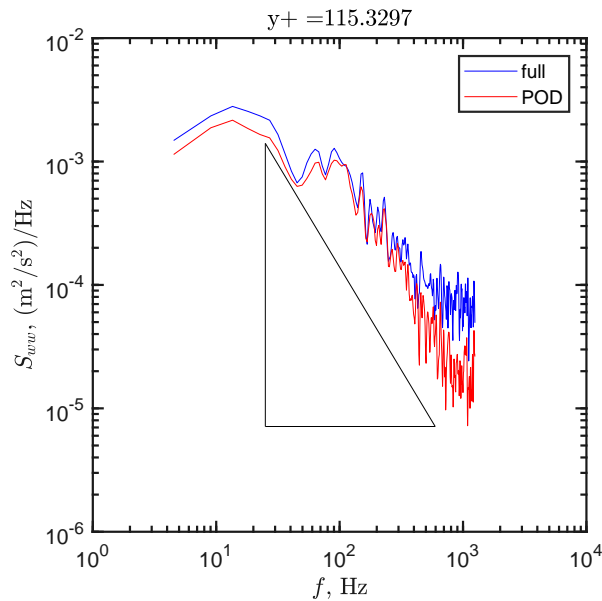


Figure 14: Power spectral density for the through-plane component of velocity for stereo PSV comparing the spectra from the velocity data to that of a reduced mode reconstruction from POD.

spectra are to be measured with stereo PIV, one would expect that stereo PSV would be able to measure the same phenomena, so long as one uses good practice to avoid the noise floor. One motivation for this is that if a PIV setup is not conducive to a particular test facility, but a PSV setup is conducive, the data could still be obtained using the stereo PSV technique with an understanding of its limitations. SPSV is not a one-to-one substitute for SPIV, but is a powerful tool for certain situations.

## REFERENCES

- Aguirre-Pablo, Andres A, Alarfaj, Meshal K, Li, Er Qiang, Hernández-Sánchez, JF & Thoroddsen, Sigurdur T 2017 Tomographic particle image velocimetry using smartphones and colored shadows. *Scientific Reports* **7**.
- Bakewell, H. P. 1966 An Experimental Investigation of the Viscous Sublayer in a Turbulent Pipe Flow. PhD thesis, Pennsylvania State University.
- Bakewell Jr, Henry P & Lumley, John L 1967 Viscous sublayer and adjacent wall region in turbulent pipe flow. *The Physics of Fluids* **10** (9), 1880–1889.
- Buchmann, Nicolas A, Willert, Christian E & Soria, Julio 2012 Pulsed, high-power led illumination for tomographic particle image velocimetry. *Experiments in fluids* **53** (5), 1545–1560.
- Chételat, Olivier & Kim, Kyung Chun 2002 Miniature particle image velocimetry system with led in-line illumination. *Measurement Science and Technology* **13** (7), 1006.
- Chevrin, Paul, Petrie, Howard & Deustch, Steven 1990 The Structure of Reynolds Stress in the Near Wall Region of a Turbulent Pipe Flow. PhD thesis, Pennsylvania State University.
- Fontaine, Arnie & Deutsch, Steven 1993 Suppression of the Near Wall Burst Process of a Fully Developed Turbulent Pipe Flow. PhD thesis, Pennsylvania State University.
- Goss, Larry & Estevadeordal, Jordi 2006 Parametric characterization for particle-shadow velocimetry (psv). In *25th AIAA Aerodynamics Measurement Technology and Ground Testing Conf. AIAA-2006 2808*.
- Goss, Larry, Estevadeordal, Jordi & Crafton, Jim 2007 Kilo-hertz color particle shadow velocimetry (psv). In *37th AIAA Fluid Dynamics Conference and Exhibit*, p. 4507.
- Hagsäter, Melker, Bruus, Henrik & Kutter, Jörg Peter 2008 Development of micro-piv techniques for applications in microfluidic systems .
- Khodaparast, Sepideh, Borhani, Navid, Tagliabue, Giulia & Thome, John Richard 2013 A micro particle shadow velocimetry ( $\mu$ psv) technique to measure flows in microchannels. *Experiments in fluids* **54** (2), 1474.
- Lindken, R & Merzkirch, W 2002 A novel piv technique for measurements in multiphase flows and its application to two-phase bubbly flows. *Experiments in fluids* **33** (6), 814–825.
- McPhail, MJ, Fontaine, AA, Krane, MH, Goss, L & Crafton, J 2015a Correcting for color crosstalk and chromatic aberration in multicolor particle shadow velocimetry. *Measurement Science and Technology* **26** (2), 025302.
- McPhail, MJ, Krane, MH, Fontaine, AA, Goss, L & Crafton, J 2015b Multicolor particle shadow accelerometry. *Measurement Science and Technology* **26** (4), 045301.
- Meinhart, CD, Wereley, ST & Gray, MHB 2000 Volume illumination for two-dimensional particle image velocimetry. *Measurement Science and Technology* **11** (6), 809.
- Olsen, MG & Adrian, RJ 2000 Out-of-focus effects on particle image visibility and correlation in microscopic particle image velocimetry. *Experiments in fluids* **29** (1), S166–S174.
- Prasad, Ajay K 2000 Stereoscopic particle image velocimetry. *Experiments in fluids* **29** (2), 103–116.
- Truong, Christine, Harris, Jeff & McPhail, Michael J 2018a The effect of out-of-plane shear within the depth of correlation in macroscopic planar particle shadow velocimetry. In *2018 AIAA Aerospace Sciences Meeting*, p. 2035.
- Truong, Christine, Hinkle, Steven S, Harris, Jeff R, Krane, Michael H, Sinding, Kyle M, Jefferies, Rhett W, Camp, Tiffany A & Fontaine, Arnie A 2018b Multiplane particle shadow velocimetry to quantify integral length scales. *Experiments in Fluids* **59** (4), 73.
- Wieneke, B. 2005 Stereo-PIV using self-calibration on particle images. *Experiments in Fluids* **39**, 267–280.
- Willert, Christian, Stasicki, Boleslaw, Klinner, Joachim & Moessner, S 2010 Pulsed operation of high-power light emitting diodes for imaging flow velocimetry. *Measurement Science and Technology* **21** (7), 075402.